Voltage-sensing domain mode shift is coupled to the activation gate by the N-terminal tail of hERG channels

Peter S. Tan, Matthew D. Perry, 1,2 Chai Ann Ng, 1,2 Jamie I. Vandenberg, 1,2 and Adam P. Hill 1,2

Human ether-a-go-go-related gene (hERG) potassium channels exhibit unique gating kinetics characterized by unusually slow activation and deactivation. The N terminus of the channel, which contains an amphipathic helix and an unstructured tail, has been shown to be involved in regulation of this slow deactivation. However, the mechanism of how this occurs and the connection between voltage-sensing domain (VSD) return and closing of the gate are unclear. To examine this relationship, we have used voltage-clamp fluorometry to simultaneously measure VSD motion and gate closure in N-terminally truncated constructs. We report that mode shifting of the hERG VSD results in a corresponding shift in the voltage-dependent equilibrium of channel closing and that at negative potentials, coupling of the mode-shifted VSD to the gate defines the rate of channel closure. Deletion of the first 25 aa from the N terminus of hERG does not alter mode shifting of the VSD but uncouples the shift from closure of the cytoplasmic gate. Based on these observations, we propose the N-terminal tail as an adaptor that couples voltage sensor return to gate closure to define slow deactivation gating in hERG channels. Furthermore, because the mode shift occurs on a time scale relevant to the cardiac action potential, we suggest a physiological role for this phenomenon in maximizing current flow through hERG channels during repolarization.

INTRODUCTION

The Journal of General Physiology

The human ether-a-go-go-related gene (hERG) encodes the pore-forming subunit of the potassium channel responsible for the cardiac delayed rectifier current (I_{Kr}) , a critical component of the repolarization phase of the cardiac action potential (Sanguinetti et al., 1995; Trudeau et al., 1995). Like all voltage-gated potassium channels, the hERG K⁺ channel is tetrameric with each subunit composed of six transmembrane domains (S1-S6). Within this arrangement, the first four transmembrane helices (S1-S4) form the voltage-sensing domain (VSD), whereas the pore domain is formed by the last two (S5 and S6) and contains the activation gate, formed at the cytoplasmic extremity of the S6 helices (Perrin et al., 2008). The general principles of electromechanical coupling are well understood. Depolarization of the transmembrane electrical potential drives outward movement of the VSD within the bilayer, and this "upward" motion pulls on the short linker between the S4 and S5 helices, the S4–S5 linker, which in turn is coupled to motion of the activation gate via specific interactions and results in channel opening (Long et al., 2005). This overall picture also holds for the hERG potassium channel (Tristani-Firouzi et al., 2002). However, despite the overall structural homology to other

voltage-gated potassium channels, hERG channels exhibit unique gating kinetics characterized by slow activation and deactivation as well as rapid, voltage-sensitive inactivation and recovery from inactivation. Notwithstanding the importance of these kinetics in determining the role of hERG in repolarization, the underlying molecular basis is poorly understood.

A particularly intriguing property of voltage gating in hERG, as well as other voltage-gated channels, is the so called mode shift of the VSD. Mode shift refers to the observation that the voltage range for VSD return is more hyperpolarized than the voltage range for upward movement of the VSD. In other words, after the VSD has moved upward, it is stabilized in the up state and therefore more energy in terms of a larger voltage gradient needs to be applied to allow return of the VSD to its resting state. This mode shift was first observed in squid axon sodium channels (Bezanilla et al., 1982) where holding the membrane potential at 0 mV for several minutes shifted the voltage range over which gating charge was transferred across the membrane by \sim 70 mV in the hyperpolarized direction relative to when the membrane was held at -90 mV. Subsequently, the same phenomenon has been observed in many other voltage-gated channels including hERG, HCN, and Shaker

¹Molecular Cardiology and Biophysics Division, Victor Chang Cardiac Research Institute, Darlinghurst, New South Wales 2010, Australia

²St. Vincent's Clinical School, University of New South Wales, Sydney, New South Wales 2052, Australia

 $Correspondence\ to\ Adam\ P.\ Hill:\ a.hill@victorchang.edu.au$

Abbreviations used in this paper: hERG, human ether-a-go-go-related gene; MTSR, methanethiosulfonate-rhodamine; PMT, photomultiplier tube; VSD, voltage-sensing domain.

^{© 2012} Tan et al. This article is distributed under the terms of an Attribution–Noncommercial–Share Alike–No Mirror Sites license for the first six months after the publication date (see http://www.rupress.org/terms). After six months it is available under a Creative Commons License (Attribution–Noncommercial–Share Alike 3.0 Unported license, as described at http://creativecommons.org/licenses/by-nc-sa/3.0/).

(Barros et al., 1997; Piper et al., 2003; Bruening-Wright and Larsson, 2007). So what is the physical basis of the mode shift? Villalba-Galea et al. (2008) reported that a VSD can exist in three states: a resting position with the VSD in the "down" state and two "up" positions. First, an active position is populated immediately after depolarization, and second, a relaxed position populated as the VSD forms additional interactions to stabilize the up conformation. It is this relaxation, as the VSD becomes stabilized in the up state, which is thought to be responsible for the mode shift.

One feature of the mode shift that is particularly variable between channel types is the time course of the voltage shift, ranging from hundreds of milliseconds in hERG (Piper et al., 2003) to seconds in Shaker (Barros et al., 1997) and minutes in sodium channels (Bezanilla et al., 1982). The observation that these time courses correlate with the rate of C-type inactivation in each of these channel types has led to the suggestion that the mode shift is related to entry into the inactivated state. Another study has suggested that the mode shift is dependent on the load placed on the VSD by the pore domain (Haddad and Blunck, 2011). In both cases, the picture is clouded by the fact that the voltage-sensitive phosphatase, ci-VSP, without a linked pore domain or a C-type inactivation process, also displays mode shifting (Villalba-Galea et al., 2008). There is therefore still some question about how and why mode shifting occurs and what determines its characteristics in different voltage-gated channels.

Given the importance of deactivation gating kinetics for the physiological role of hERG K⁺ channels in cardiac repolarization, we have investigated how hERG deactivation is modulated by mode shifting of the VSD. Previous studies have identified the cytoplasmic N-terminal domain of hERG as a critical factor regulating channel deactivation (Morais Cabral et al., 1998; Wang et al., 1998). Furthermore, it has been shown that deletion of just the distal N-terminal tail, either amino acids 2–25 (Ng et al., 2011) or 2–12 (Wang et al., 1998), completely recapitulated the accelerated deactivation phenotype observed with truncations of a majority of the N-terminal cytoplasmic domain. It has also been suggested that the N-terminal tail may interact with the S4-S5 linker to modulate deactivation of hERG (Li et al., 2010; De la Peña et al., 2011). We therefore hypothesized that truncation of the N-terminal tail could be affecting the VSD mode shift. In this study, we have measured VSD movement using voltage-clamp fluorometry and ionic current flow to investigate the role of the N-terminal tail in mode shifting. Although modification of the N-terminal tail, either through truncation or point mutation, does not alter the VSD mode shift, it does uncouple the shift from closure of the cytoplasmic gate, suggesting a crucial role for the N-terminal tail in coupling channel closure to VSD return. This is a

phenomenon that has not been reported for other voltage-gated channels that provides insight into the unique deactivation properties of hERG channels.

MATERIALS AND METHODS

Molecular biology

hERG cDNA (a gift from G. Robertson, University of Wisconsin, Madison, WI) was subcloned into a pBluescript vector containing the 5' and 3' untranslated regions of the Xenopus laevis β globin gene (a gift from R. Vandenberg, University of Sydney, Sydney, New South Wales, Australia). Mutagenesis was performed using the QuikChange mutagenesis method (Agilent Technologies) and was confirmed by DNA sequencing. The E518C mutation in the S3–S4 linker was introduced as a site for fluorophore labeling. Two native extracellular cysteine residues (C445 and C449 in the S1-S2 linker) were removed and replaced with serine residues to prevent mistargeted labeling. This construct (C445S:C449S:E518C) will be referred to as E518C throughout the manuscript. In experiments involving acquisition of fluorescent signals as a measure of VSD movement, this construct is representative of wild-type hERG. Mutant channel cDNAs were linearized with BamHI and cRNA transcribed with T7 RNA polymerase using the mMessage mMachine kit (Ambion).

Oocyte preparation

Xenopus oocytes were prepared as previously described (Clarke et al., 2006). Stage V and VI oocytes were isolated, stored in tissue culture dishes containing ND96 (2.0 mM KCl, 96.0 mM NaCl, 1.8 mM CaCl₂, 1.0 mM MgCl₂, and 5.0 mM HEPES) supplemented with 2.5 mM sodium pyruvate, 0.5 mM theophylline, and 10 μg/ml gentamicin, adjusted to pH 7.5 with NaOH, and incubated at 17°C. All experiments were approved by the Garvan/St. Vincent's Animal Ethics Committee (approval ID 08/34). Xenopus oocytes were injected with 5–10 ng cRNA and incubated at 17°C for 24–48 h before electrophysiological recordings and up to 72 h for fluorescent experiments.

Electrophysiology

All experiments were undertaken at room temperature (21–22°C). Two-electrode, voltage-clamp experiments were performed using a GeneClamp 500B amplifier (Molecular Devices). Glass microelectrodes had tip resistances of 0.3–1.0 M Ω when filled with 3 M KCl. Oocytes were perfused with ND96 solution (see previous section). In all protocols, a step depolarization of 10 mV from the holding potential of -90 mV was applied at the start of each sweep to enable offline leak current subtraction. We assumed that the current leakage was linear in the voltage range -160 to 80 mV. Data acquisition and analysis were performed using pCLAMP (version 9.2; Molecular Devices) and Excel (Microsoft) software.

For fluorometry experiments, we tested labeling at several positions in this region, and although all positions gave signals with comparable characteristics, we found that methanethiosulfonaterhodamine (MTSR; Toronto Research Chemicals) labeling of position 518C gave the most reproducible and consistent results and so was chosen for this study. A summary of MTSR fluorescent reports from other positions (Fig. S1) as well as TMRM (tetramethylrhodamine maleimide) fluorescent reports from 518C (Fig. S2) is presented in the Supplemental material. Oocytes were labeled with 5 µM MTSR in a depolarizing solution (98 mM KCl, 1 mM MgCl₂, 2 mM CaCl₂, and 5 mM HEPES, pH 7.4) for 1 min on ice in the dark. Experiments were performed on the stage of an Eclipse Ti-U inverted microscope (Nikon) with epifluorescent attachment. MTSR has a maximum for light absorption at 565 nm

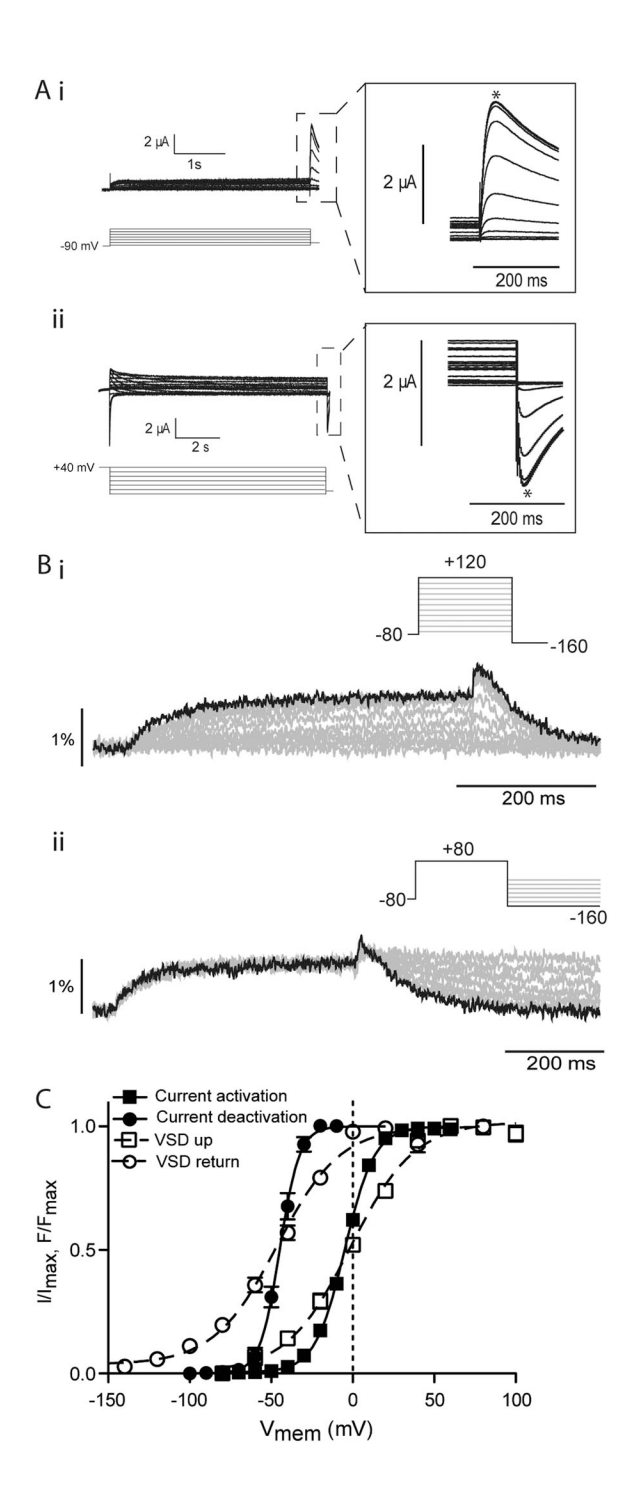


Figure 1. Mode shift of hERG channels. (A) Example traces recorded in response to protocols shown to measure the voltage-dependent equilibria of activation (i) and deactivation (ii) of E518C hERG channels. Insets are expansions of the highlighted regions. Peak currents were measured at the points marked with asterisks. (B) Example fluorescent traces recorded from MTSR-labeled 518C using voltage-clamp fluorometry in response to the protocols shown to measure activation/upward motion (i) and return (ii) of the VSD of E518C hERG. (C) Summary of voltage dependence of equilibria of activation and deactivation. Solid lines are fits of the Boltzmann equation to current data, whereas broken lines are fits of the Boltzmann equation to the fluorescent data. $V_{0.5}$ values were -4 ± 0.9 mV and -44 ± 2 mV for current activation and deactivation, respectively (SEM; n=10) and 1.4 ± 2 mV

and a maximal emission at 586 nm. The dye was excited with light produced by a super high pressure mercury lamp (model HB-10104AF; Nikon) filtered through a 525-nm band pass excitation filter and passed via a dichroic mirror and 40× objective (CFI Plan Apochromat 40×, numerical aperture 0.95; Nikon) to the oocyte in the bath chamber. Fluorescence emission was collected via the same high NA 40× objective and filtered through a 565-nm long pass emission filter before being passed to a 9124b Electron Tubes photomultiplier tube (PMT) module (Cairn Research) attached to the auxiliary port of the microscope. Voltage signals from the PMT were filtered and/or amplified using an Integra PMT Controller (Cairn Research) and then digitized using an Axon Digidata 1322 A/D converter (Molecular Devices) and acquired simultaneously with the current record on a computer running pCLAMP 9.2 software.

Data analysis

The voltage dependence of the distribution between open and closed states depends on whether the channels start from the closed state or whether they start from the open state. To distinguish between them in our analysis of ionic currents, we refer to the scenario of channels starting in the closed state as being "steady-state activation," whereas when the channels start in the open state we refer to that as "steady-state deactivation." For analysis of steady-state activation and deactivation as well as the voltage-dependent distributions of VSD movement, data were acquired using experimental protocols shown in individual figures and fitted with a Boltzmann function:

$$I / I_{\text{max}} = \left[1 + \exp^{\frac{V_{0.5} - V_t}{k}}\right]^{-1},$$

where I/I_{max} is the relative conductance, $V_{0.5}$ is the half-activation potential, V_i is the test voltage, and k is the slope factor. In experiments in which the free energies associated with voltage-dependent activation or deactivation were examined, the same datasets were fitted with the thermodynamic form of the Boltzmann equation:

$$I/I_{\text{max}} = \left[1 + \exp^{\frac{\Delta G_0 - z_g EF}{RT}}\right]^{-1},$$

where ΔG_0 is the work done at 0 mV, z_g is the effective number of gating charges moving across the electric field, E, F is Faraday's constant, R is the universal gas constant, and T is the absolute temperature.

Online supplemental material

Fig. S1 shows comparisons of the voltage-dependent equilibria of current activation and VSD upward motion for MTSR-labeled E518C, E519C, and L520C hERG channels. Fig. S2 shows a biphasic fluorescent profile for TMRM-labeled 518C hERG. Fig. S3 shows the effect of N-terminal truncation on mode shift of ionic current in wild-type hERG. Table S1 is a summary of parameters for Boltzmann fits to the voltage-dependent equilibria of ionic current activation and deactivation for the alanine scan of the hERG N terminus. Online supplemental material is available at http://www.jgp.org/cgi/content/full/jgp.201110761/DC1.

and -50.9 ± 1 mV for upward motion and return of the VSD, respectively (SEM; n = 12).

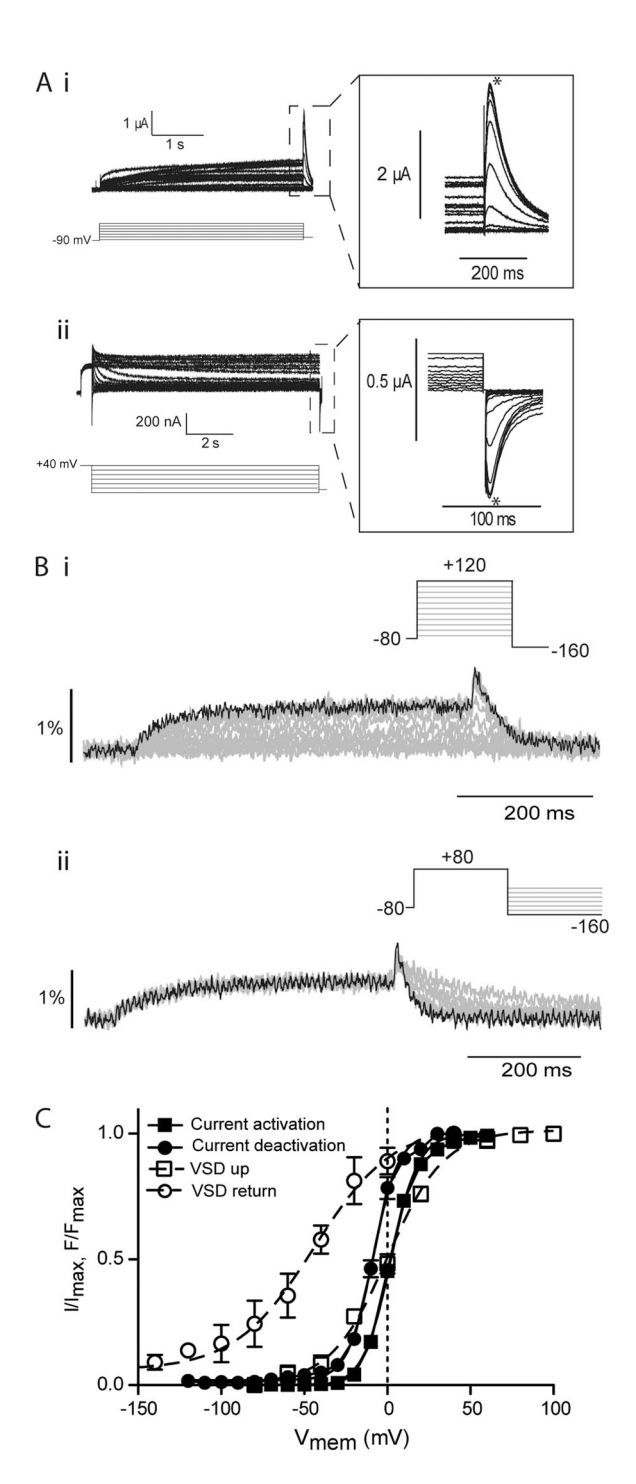


Figure 2. Effect of N-terminal truncation on mode shift of hERG channels. (A) Example traces recorded in response to protocols shown to measure the voltage-dependent equilibria of activation (i) and deactivation (ii) of $\Delta 2$ –25 hERG channels. Insets are expansions of the highlighted regions. Peak currents were measured at the points marked with asterisks. (B) Example fluorescent traces recorded using voltage-clamp fluorometry in response to the protocols shown to measure activation/upward motion (i) and return (ii) of the VSD of $\Delta 2$ –25 hERG. (C) Summary of voltage dependence of equilibria of activation and deactivation. Solid lines are fits of the Boltzmann equation to current data, whereas broken lines are fits of the Boltzmann equation to the fluorescent data. $V_{0.5}$ values were 2 ± 0.3 mV and -10 ± 0.4 mV for current activation and deactivation, respectively (SEM; n = 7).

RESULTS

Mode shift in hERG channel gating

Mode shifting of the hERG VSD has previously been demonstrated using measurements of gating currents (Piper et al., 2003) though no effect has been reported on ionic currents, i.e., a hyperpolarized shift of deactivation (gate closing) relative to activation (gate opening). Fig. 1 A shows typical examples of current families recorded from E518C hERG channels (representative of wild type [see Materials and methods]) using protocols to measure steady-state activation ($V_{0.5,-90}$, measured from a holding potential of -90 mV) and deactivation ($V_{0.5, 40}$, measured from a holding potential of 40 mV). The $V_{0.5}$ values for steady-state activation and deactivation were measured as -4.0 ± 0.9 mV and $-44.8 \pm$ 0.2 mV (SEM; n = 10), respectively (Fig. 1 C). This shift in the voltage dependence of steady-state deactivation compared with activation is consistent with the mode shift observed previously for hERG gating currents (Piper et al., 2003) and is similar in magnitude to that measured for other ion channels (Wonderlin and Strobl, 1996; Barros et al., 1997). To examine VSD movement associated with this mode shift of ionic current, we used voltage-clamp fluorometry. Fig. 1 B shows representative fluorescent traces recorded from MTSRlabeled E518C hERG channels in response to protocols to measure the voltage-dependent equilibria of VSD upward motion/activation (Fig. 1 B, i) and VSD return (Fig. 1 B, ii). For VSD activation, the peak fluorescent response during the test pulse was plotted against voltage to give representation of voltage-dependent movement of the VSD during the activation process and fitted with the Boltzmann function. For deactivation, the decaying phase of the fluorescent record during the test pulse was fitted with exponential functions and extrapolated to their plateau. This steady-state value was then plotted against the test pulse voltage and fitted with the Boltzmann function. The midpoints for VSD activation and return were -1.4 ± 2 mV and -46.4 ± 1 mV, respectively (SEM; n = 12), indicating the VSD mode shift paralleled that measured in the ionic current records for E518C channels (Fig. 1 C).

Effect of N-terminal truncation on hERG mode shift

The aforementioned analysis shows a clear hyperpolarized shift in the voltage dependence of steady-state deactivation compared with activation for E518C channels and a corresponding shift in VSD return relative to VSD upward movement. This is consistent with the concept of a mode shift occurring as the VSD is stabilized in the up conformation. Fig. 2 illustrates the

 $V_{0.5}$ values were measured as 0 ± 1 mV (SEM; n = 8) and -43 ± 7 mV (SEM; n = 11) for activation and return of the VSD, respectively.

same analysis of ionic current and VSD movement in $\Delta 2$ –25 truncated hERG channels. Typical examples of families of ionic currents and representative fluorescent traces from the truncated hERG constructs are shown in Fig. 2 (A and B, respectively). The midpoint of steady-state activation for $\Delta 2$ –25 only differed from E518C by a small but significant amount ($V_{0.5,-90}$ 2 ± 0.3 mV, SEM; n = 7; Student's t test, P < 0.05), whereas the $V_{0.5}$ of steady-state deactivation of the N-terminally truncated construct was shifted \sim 35 mV in the depolarized direction relative to E518C ($V_{0.5, 40}$ -8.0 ± 0.3 mV, SEM; n = 7; Fig. 2 C). Therefore, in the $\Delta 2-25$ construct, the mode shift of ionic current has been dramatically reduced. It should be noted that the $\Delta 2$ –25 truncation resulted in similar changes in the wild-type background to those observed in the E518C (Fig. S3), illustrating that these effects are a function of the deletion of the N-terminal tail and not a property of the E518C background.

This reduction in the hyperpolarized shift in steady-state deactivation relative to activation observed in the $\Delta 2$ –25 background suggests that either (a) deletion of the first N-terminal 25 aa of hERG reduces the VSD mode shift or (b) VSD mode shift could still be occurring but is no longer translated to the gate. Analysis of fluorescent records from MTSR-labeled $\Delta 2$ –25 channels showed that upward movement of the VSD occurred over the same voltage range as in E518C ($V_{0.5}$ 0.0 ± 1.0 mV, SEM; $N_{0.5}$ and VSD return was still shifted in the hyperpolarized direction ($V_{0.5}$ –44.0 ± 5.0 mV, SEM; $N_{0.5}$ = 13), demonstrating that VSD mode shifting was still intact. These data therefore suggest that N-terminal deletion in hERG uncouples the VSD mode shift from the S6 activation/deactivation gate.

Kinetic effects of N-terminal truncation in hERG channels To further interrogate the relationship between VSD motion and opening/closing of the activation gate in the context of mode shifting, we examined the kinetics of the processes. The effects of the N-terminal deletion on the rates of ionic current activation and VSD upward motion are shown in Fig. 3. Electrophysiological records measured in response to standard envelope of tails protocols were acquired (Fig. 3A), and the data were fitted with exponential functions to derive the time constants for activation of ionic current (τ_{act}) , which are reflective of the rate of opening of the cytoplasmic gate (Fig. 3 B). Over the voltage range tested, the effect of the $\Delta 2$ –25 truncation on the rates of activation was minimal (Fig. 3 C), causing a slight but significant deceleration of the rate of opening of the gate at some potentials, with no significant effect at others. Likewise, the time constants of upward motion of the voltage sensor measured from the fluorescent signal are summarized in Fig. 3 D and show a similar pattern, that is, either no effect or a

slight deceleration depending on the membrane voltage.

Collectively with the equilibrium activation data, these data suggest that the N-terminal tail does not play a major role in hERG activation.

We next examined the relationship between VSD return and closing of the gate. In a previous publication we have reported the effects of the $\Delta 2$ –25 truncation on the rate of current deactivation and showed that the truncation accelerates both the fast and slow time constants (τ_{fast} and τ_{slow}) and that the fast component was the dominant factor in the rate of deactivation at negative potentials for both wild-type and truncated hERG (Ng et al., 2011). In this study, we have therefore only examined the fast time constant (τ_{fast}). Fig. 4 A shows representative current (Fig. 4 A, i) and fluorescent records (Fig. 4 A, ii) for MTSR-labeled E518C and $\Delta 2$ –25

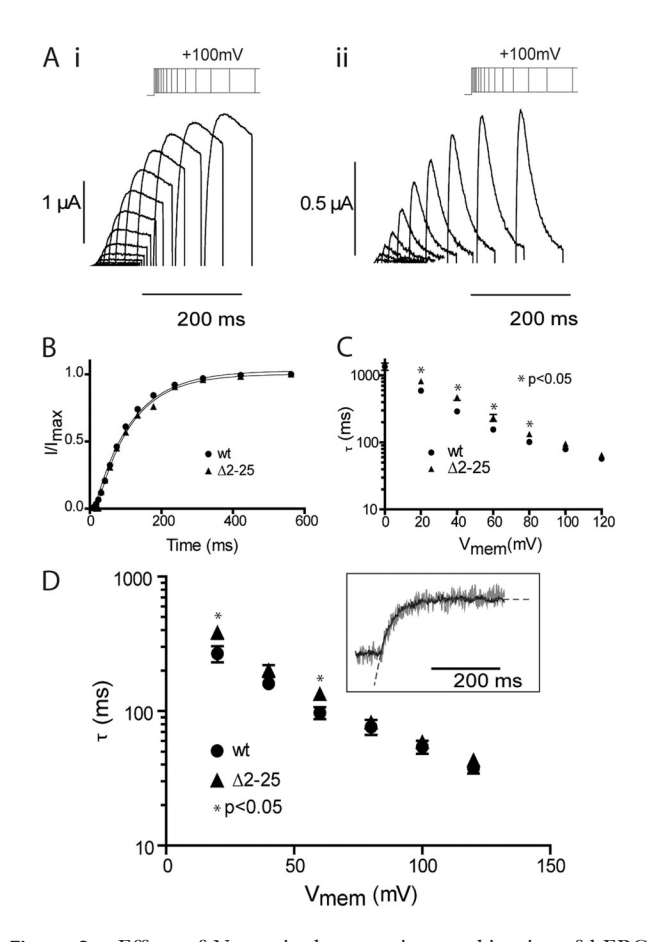


Figure 3. Effect of N-terminal truncation on kinetics of hERG activation. (A) Typical examples of currents recorded in response to the envelope of tails protocols shown for E518C (i) and $\Delta 2$ –25 (ii) hERG channels. In these examples, the activating potential was 100 mV. (B) Peak tail currents plotted against the duration of the activating pulse for the examples shown in A. The black line is a fit of a single exponential to the activation time course. (C) Summary of the voltage dependence of rates of activation of ionic current. Error bars are SEM; $n \geq 8$. (D) Summary of the voltage dependence of the rates of VSD activation/upward motion derived from single exponential fits to the fluorescent time course using the same protocol illustrated in Fig. 1 B (i). Error bars are SEM; $n \geq 7$. The inset shows example fits to fluorescent traces from MTSR-labeled E518C recorded at 100 mV.

hERG at a test potential of -120 mV. The decay of the current traces and fluorescent records were both fitted with exponential functions to extract the time constants defining gate closure and VSD return, respectively. The voltage dependence of this relationship is summarized in Fig. 4 B. In E518C, the fast component of current deactivation overlays the rate of VSD return over the entire range of voltages tested. This is consistent with return of the VSD defining the fast component of deactivation in hERG, and moreover, at negative voltages, where $\tau_{\rm fast}$ is dominant, this is the rate-limiting step for closure of the gate.

Fig. 4 B also illustrates the effects of the $\Delta 2$ –25 truncation on the kinetics of gate closure and VSD return, showing that the effect on the two processes is markedly different. Although the former is \sim 6-fold faster in $\Delta 2$ –25, the latter is only modestly accelerated by \sim 1.5–2-fold. These data show that in the background of the truncation, the rate of VSD return is no longer the limiting factor for deactivation of ionic current (the gate closes much faster than the VSD returns at all voltages tested) and provide further evidence that the N-terminal tail couples the VSD to the gate during deactivation and deletion of the N-terminal uncouples this process.

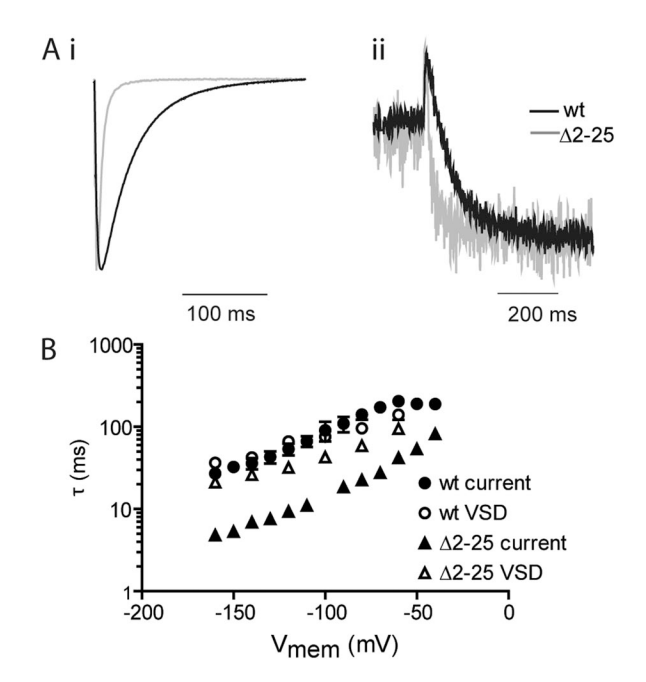


Figure 4. Effect of N-terminal truncation on kinetics of hERG deactivation. (A) Typical examples of ionic current (i) and fluorescence (ii) recorded after repolarization to -120 mV from a depolarized holding potential for E518C and $\Delta 2$ –25 hERG. The fast time constant (τ_{fast}) for deactivation of ionic current was derived from a fit of a double exponential function to the decaying phase of the current after repolarization. Time constants for VSD return were derived from fits of a single exponential to the decaying phase of the fluorescence record. (B) Summary of the voltage dependence of rates of deactivation and VSD return for E518C and $\Delta 2$ –25 hERG channels. Error bars are SEM; $n \geq 7$.

Molecular basis of coupling of VSD to gate closing

Our experiments involving $\Delta 2$ –25 truncated hERG channels showed that this region couples VSD return to closing of the gate to define the voltage sensitivity and rate of channel deactivation. To identify the specific molecular players involved in coupling, we performed an alanine scan of the N terminus of wild-type hERG. For each alanine mutant, we recorded ionic currents to measure steady-state activation and deactivation (Fig. 5 A) as previously described in Figs. 1 and 2. Example analyses illustrating the effects of the alanine mutants at positions R4, R5, and G6 on steady-state activation and deactivation of ionic current are shown in Fig. 5 B. These datasets were fitted with the thermodynamic form of the Boltzmann equation (see Materials and methods), and $\Delta\Delta G_0$, the difference between the free energy terms associated with activation ($\Delta G_{0, act}$) and deactivation ($\Delta G_{0, \text{deact}}$) was calculated for each mutant. The full set of $V_{0.5}$ as well as ΔG_0 for voltage-dependent activation and deactivation of ionic currents is presented in Table S1. Fig. 5 C illustrates the change in $\Delta\Delta G_0$ caused by each alanine mutant relative to wildtype hERG (termed $\Delta\Delta\Delta G_0$ on the y axis of Fig. 5 C). This measure of the change in the difference between the voltage-dependent equilibrium of deactivation relative to activation is a simple measure of the effect of the mutation on the magnitude of the mode shift of ionic current. It is clear from Fig. 5 C that there is a delineation of the effects of the mutants between the first 9 aa (which we have previously identified as the unstructured tail) and amino acids 10-25 (which we have shown forms an α helix [Ng et al., 2011]). In particular, mutation of three amino acid residues in this region, R4A, R5A, and G6A, contributes strongly to coupling with $\Delta\Delta\Delta G_0$ of ~ 3 kcal/mol. The clustering of these three residues in the unstructured tail suggests that this is the effector region for coupling the VSD to the cytoplasmic gate during deactivation and is consistent with these residues being the molecular players defining the effect of the $\Delta 2$ –25 truncation.

To confirm that these residues are indeed the molecular determinants of coupling of VSD return to closing of the cytoplasmic gate by the N-terminal tail, we again used voltage-clamp fluorometry. If closing of the gate has become uncoupled from return of the VSD, we would expect to see normal VSD mode shift, reported by the fluorescent change, in the same manner as we have already demonstrated for the $\Delta 2$ –25 truncation. That is, the hyperpolarized shift of VSD return relative to VSD upward motion should be the same in the mutants as in the wild type. Fig. 6 A illustrates steady-state activation and deactivation of ionic current for the three point mutants identified in Fig. 5 in the background of E518C (to enable labeling with MTSR). In exactly the same manner as illustrated for the $\Delta 2-25$ truncation (Fig. 2 and Fig. S3), the overall equilibria of

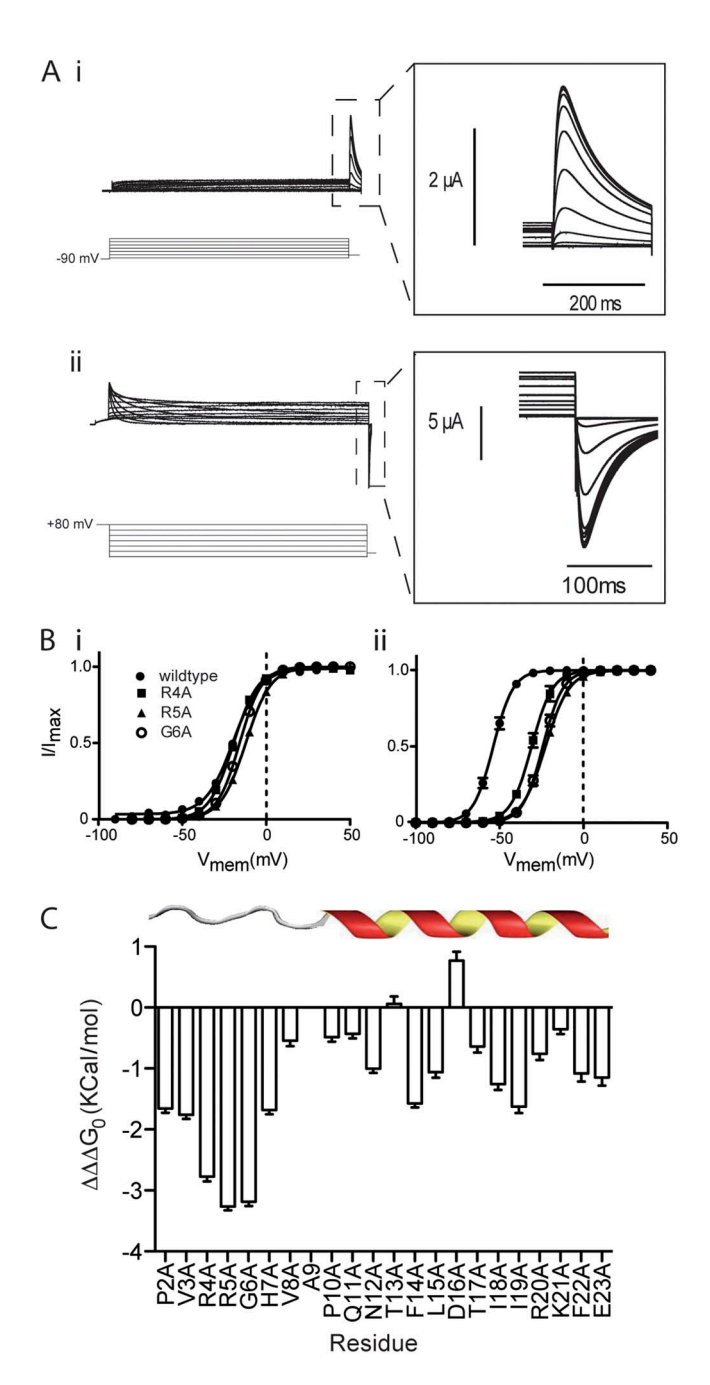


Figure 5. Alanine scan of N-terminal tail. (A) Example traces recorded in response to protocols shown to measure the voltagedependent equilibria of activation (i) and deactivation (ii) ionic current in R4A hERG channels. Insets are expansions of the highlighted regions. (B) Summary of voltage-dependent equilibria of activation (i) and deactivation (ii) for R4A, R5A, and G6A mutants. Solid lines are fits of the Boltzmann equation to data. $V_{0.5}$ values for activation were measured as 3.7 ± 1.1 mV, 2.8 ± 1.3 mV, and -3.4 ± 1.5 mV for R4A, R5A, and G6A, respectively (SEM; n > 4). For deactivation of ionic current, $V_{0.5}$ values were measured as -19.3 ± 2.5 mV, -10 ± 0.9 mV, and -16.1 ± 1.2 mV for R4A, R5A, and G6A, respectively (SEM; n > 5). (C) Mutation-dependent changes (termed $\Delta\Delta\Delta G_0$) in the difference ($\Delta\Delta G_0$) between the free energy terms associated with the voltage-dependent equilibrium of deactivation ($\Delta G_{0, \text{deact}}$) and activation ($\Delta G_{0, \text{act}}$) relative to wild-type hERG (SEM; $n \ge 21$). Three amino acid residues in this

activation and deactivation are shifted in the depolarized direction in this background, but the relative effects of each of the mutants remain the same as in the wild-type background illustrated in Fig. 5 B. Specifically, R4A and R5A had a small but significant effect on the midpoint of steady-state activation ($V_{0.5}$ 3.7 ± 1.1 mV and 2.8 ± 1.3 mV, SEM; n > 4) for R4A and R5A, respectively, compared with -4 ± 0.9 mV (SEM; n = 10) for 518C, whereas G6A was not significantly different from E518C ($V_{0.5}$ – 3.4 ± 1.5 mV, SEM; n = 6; one-way ANOVA, Dunnett's post test, P < 0.05). In contrast, midpoints of steady-state of deactivation for R4A (-19.3 ± 2.5 mV, SEM; n = 7), R5A (-10 ± 0.9 mV, SEM; n = 4), and G6A $(-16.1\pm 1.2 \text{ mV}, \text{ SEM}; n = 5)$ were all significantly shifted in the depolarized direction relative to E518C $(-44.8 \pm 0.2 \text{ mV}, \text{SEM}; n = 10; \text{one-way ANOVA, Dunnett's})$ post test, P < 0.05).

Having demonstrated that the effect of these mutants is the same in either the wild-type or E518C background, we examined VSD motion for each of the three point mutants. Fig. 6 B shows examples of fluorescent records measured from MTSR-labeled R4A channels in response to protocols to measure the voltage-dependent equilibria of VSD upward motion and VSD return, as previously described in Figs. 1 and 2. These data are summarized in Fig. 6 C for E518C and each of the three point mutants. $V_{0.5}$ values for VSD upward motion were -1.4 ± 2 mV, 20.9 ± 2.6 mV, 10.0 ± 3.5 mV, and 6.2 ± 3.8 mV for 518C, R4A, R5A, and G6A, respectively (SEM; n > 4). These depolarized shifts in VSD upward motion are consistent with the shifts in current activation observed in this background (Fig. 6 A). $V_{0.5}$ values for VSD return were -46.4 ± 1 mV, -34.5 ± 7.2 mV, $-29.6 \pm$ 3.8 mV, and $-29.0 \pm 4.4 \text{ mV}$ for E518C, R4A, R5A, and G6A, respectively (SEM; n > 4). To compare the magnitude of the mode shift of ionic current and VSD motion, the datasets in Fig. 6 (A and C) were fitted with the thermodynamic form of the Boltzmann equation, and just as in Fig. 5, $\Delta\Delta G_0$, the difference between the free energy terms associated with activation/VSD upward motion ($\Delta G_{0, act}$) and deactivation/VSD return ($\Delta G_{0, deact}$), was calculated for each mutant. This value is a measure of the difference in the voltage-dependent equilibria for deactivation/VSD return relative to activation/ VSD upward motion and so is a simple measure of the mode shift. Fig. 6 D shows that although each of the mutants significantly reduced the mode shift of ionic current (one-way ANOVA, Dunnett's post test, P < 0.05), none of them reduced the mode shift of the VSD. Because these observations parallel those in the $\Delta 2$ –25 truncation, they confirm that these residues are the molecular determinants of coupling of the cytoplasmic gate to

region, R4A, R5A, and G6A, contribute strongly to coupling with $\Delta\Delta\Delta G_0$ of \sim 3 kcal/mol.

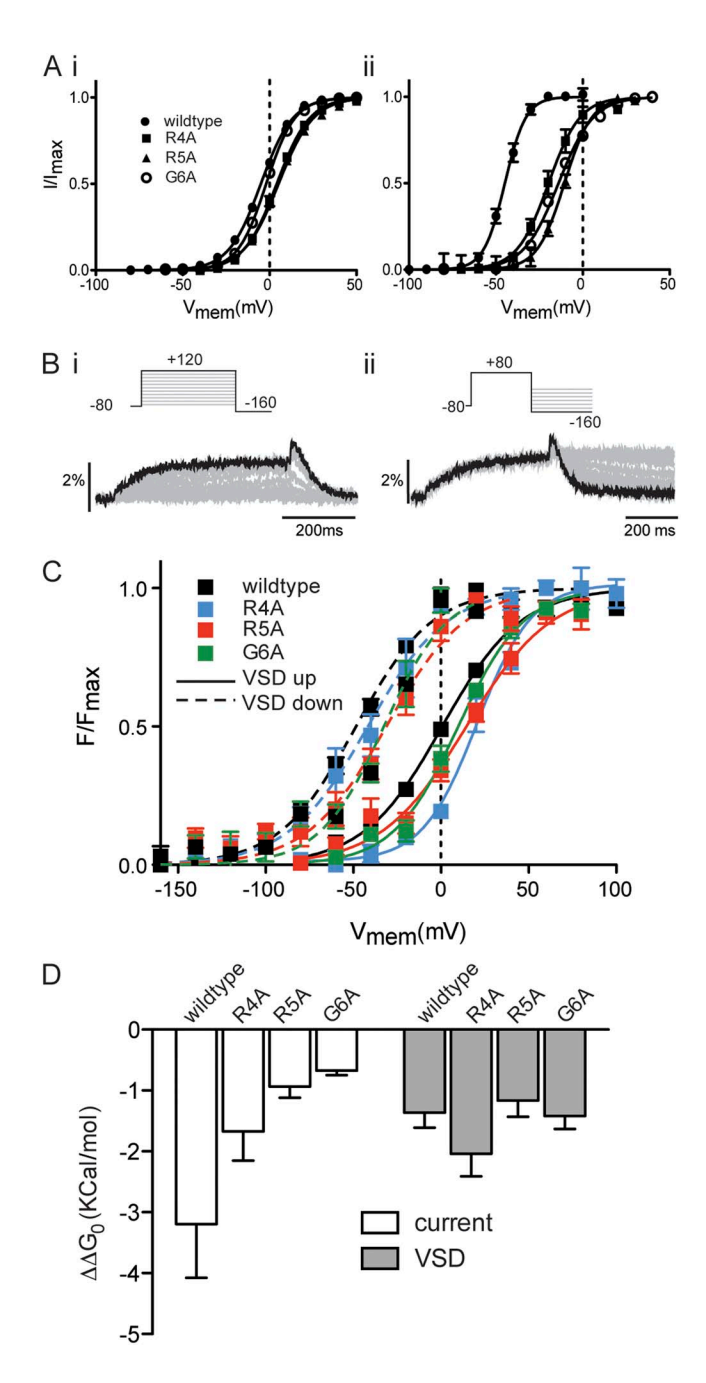


Figure 6. Voltage-clamp fluorometry of residues contributing to coupling. (A) Summary of the voltage-dependent equilibria of activation (i) and deactivation (ii) of ionic current for R4A, R5A, and G6A mutants in the E518C background. Solid lines are fits of the Boltzmann equation to data. (B) Example fluorescent traces recorded from MTSR-labeled R4A E518C hERG using voltageclamp fluorometry in response to the protocols shown to measure upward motion (i) and return (ii) of the VSD. (C) Summary of the voltage-dependent equilibria of VSD upward motion and return. $V_{0.5}$ values for VSD upward motion were -1.4 ± 2 mV, 20.9 ± 1.0 2.6 mV, $10 \pm 3.5 \text{ mV}$, and $6.2 \pm 3.8 \text{ mV}$ for E518C, R4A, R5A, and G6A, respectively (SEM; n > 4). $V_{0.5}$ values for VSD return were -46.4 ± 1 mV, -34.5 ± 7.2 mV, -29.6 ± 3.8 mV, and -29.0 ± 4.4 mV for E518C, R4A, R5A, and G6A, respectively (SEM; n > 4). (D) Difference between free energy terms ($\Delta \Delta G_0$) associated with the voltage-dependent equilibrium of current deactivation

VSD return. It should be noted that although R5A and G6A were not significantly different from wild-type, R4A actually had a larger $\Delta\Delta G_0$ that would be consistent with an increased VSD mode shift of the VSD. We are currently unable to explain this observation, which may occur as a result of mutation-specific interactions in the region of the N-terminal tail. Nevertheless, in all the point mutants, the mode-shifted VSD is clearly uncoupled from the cytoplasmic gate.

Link between C-type inactivation and mode shift

Our results show that in wild-type channels, the modeshifted VSD is coupled to closing of the cytoplasmic gate via the N terminus of the channel. However, in addition to this coupling to downstream deactivation events, a previous study has suggested that mode shifting of the VSD is coupled to upstream C-type inactivation events as a prerequisite for the mode shift to occur (Olcese et al., 1997). However, another study has shown that VSD mode shift is unaltered in inactivation-deficient channels (Piper et al., 2003). To investigate this phenomenon, we examined the voltage dependence of the activation and deactivation of ionic current in the inactivation-deficient S631A hERG mutant. Fig. 7 A shows currents recorded to measure steady-state activation and deactivation of S631A channels, whereas the voltage dependence of these gating processes are illustrated in Fig. 7 B. Neither the $V_{0.5}$ values for activation $(-20.32 \pm 0.5 \text{ mV} \text{ and } -21.7 \pm 0.7 \text{ mV} \text{ for wild type})$ and S631A, respectively, SEM; $n \ge 5$) nor deactivation $(-54.9 \pm 1.6 \text{ mV} \text{ and } -50.72 \pm 0.9 \text{ mV} \text{ for wild type}$ and S631A, respectively, SEM; n = 4) of ionic current were significantly different (Student's t test, P < 0.05). These data suggest that the lack of C-type inactivation, at least as a result of the S631A mutant, does not affect mode shifting.

DISCUSSION

In this study, we examined the role of the N-terminal tail of the hERG channel in VSD mode shifting and it's coupling to the activation gate to regulate current. Our data show that deletion of the first 25 aa from the N-terminal tail of the hERG channel accelerates deactivation through a process of uncoupling gate closure from VSD motion, whereas under wild-type conditions, the rate of VSD return acts as the rate-limiting component at negative potentials. At the molecular level, this coupling of the VSD to the gate is defined by a triplet of amino acid residues at positions R4, R5, and G6 in the unstructured region of the N-terminal tail. Furthermore, we show that in N-terminally modified channels,

relative to current activation (open) and VSD return relative to VSD upward motion (gray; SEM; $n \ge 6$).

VSD mode shifting still occurs, but this is uncoupled from the activation gate, the first time this has been observed in a voltage-gated channel.

Mode shifting in hERG channels

One of the defining features of hERG channel gating is the slow kinetics of the activation/deactivation process. Although activation/deactivation typically occurs over tens of milliseconds in voltage-gated potassium channels, in hERG this process is one to two orders of magnitude slower (Wang et al., 1997). Several studies have

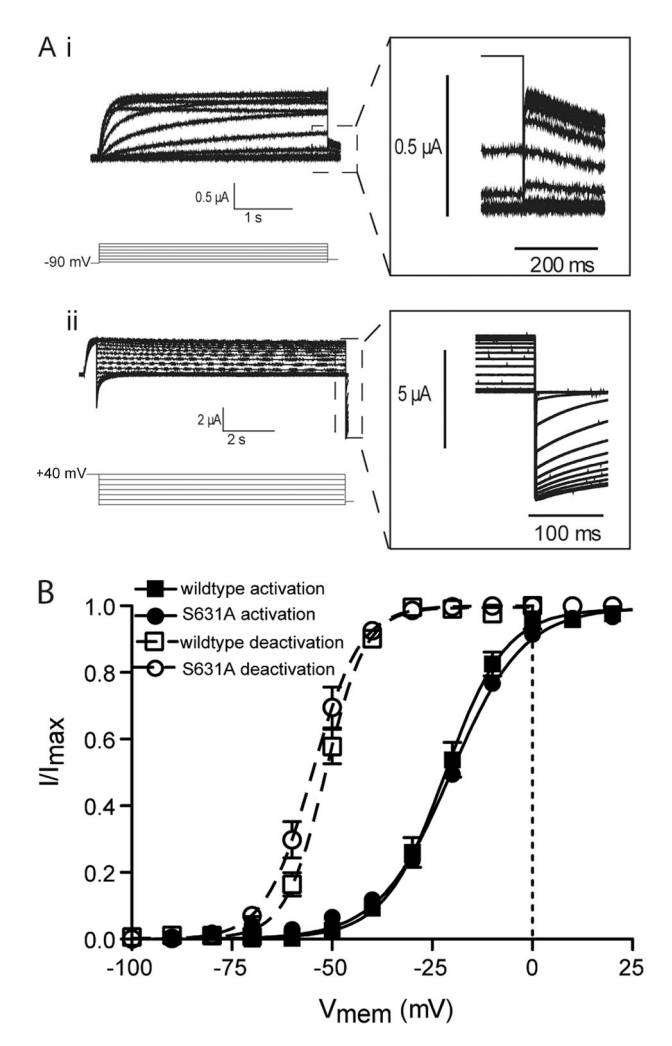


Figure 7. Mode shift of ionic current in S631A hERG. (A) Example traces recorded in response to the protocols shown to measure the voltage-dependent equilibria of activation (i) and deactivation (ii) of ionic current in inactivation-deficient S631A hERG channels. Insets are expansions of the highlighted regions. (B) Summary of the voltage-dependent equilibria of activation and deactivation. Solid lines are fits of the Boltzmann equation to activation data, whereas broken lines are fits of the Boltzmann equation to the deactivation data. Neither the $V_{0.5}$ values for activation (-20.32 ± 0.5 mV and -21.7 ± 0.7 mV for wild type and S631A, respectively, SEM; $n \ge 5$) nor deactivation (-54.9 ± 1.6 mV and -50.72 ± 0.9 mV for wild type and S631A, respectively, SEM; n = 4) were significantly different from wild type (Student's t test, P < 0.05).

previously used voltage-clamp fluorometry to investigate the voltage sensitivity of VSD movement in hERG and other voltage-gated potassium channels (Smith and Yellen, 2002; Pathak et al., 2007; Van Slyke et al., 2010). These studies showed that upward motion of the VSD occurs over an overlapping range of transmembrane potentials with activation of ionic current and suggested that in hERG slow VSD movement is the rate-determining step in slow activation. In agreement with these findings, gating charge measurements showed that the bulk of charge movement associated with the hERG voltage sensor movement is slow (Piper et al., 2003). The data we present here corroborate these previous observations. During activation, VSD movement is slow, on a time scale consistent with opening of the channel, and occurs at overlapping voltages. Moreover, we show that deletion of the first 25 aa from the N terminus of the hERG channel has little or no effect on the voltage dependence or rates of either VSD activation or gate opening.

In contrast to the multiple studies concerning activation, there have been no previous studies directly examining the relationship between VSD return and current deactivation in hERG or the molecular players involved in coupling and control of this process. Piper et al. (2003) measured gating charges associated with VSD upward motion (from holding potentials of −110 mV) and VSD return (from holding potentials of 0 mV), showing the latter was shifted in the hyperpolarized direction. They did not however examine the voltage dependence of the corresponding ionic currents. Our data show that currents elicited from a depolarized holding potential, describing closing of the hERG channel, occur with a midpoint of the voltage-dependent equilibrium shifted ~40 mV in the hyperpolarized direction relative to channel opening. This is characteristic of the mode shift observed in a range of voltagegated channels (Wonderlin and Strobl, 1996; Barros et al., 1997). The magnitude of the shift has been shown to be dependent on both the value and duration of the initial holding pulse. For example, in Shaker channels, where the mode shift has been best characterized, the shift occurs with a biexponential time course described by time constants of 4.1 s and 24 s at 0 mV (Barros et al., 1997). Our data suggest that in hERG the process is faster because the 40-mV shift we report has occurred after just 500-ms depolarization. Although the kinetics of mode shifting was not a focus of this study, this faster time course in hERG is consistent with the concept of mode shifting being related to C-type inactivation, which occurs much faster in hERG channels than is typically found in other voltage-gated potassium channels (milliseconds compared with seconds; Smith et al., 1996; Spector et al., 1996). However, our data also indicate that in inactivation-deficient S631A hERG channels, the same mode shift still occurs as in wild-type hERG. This matches the previous observation by Piper et al. (2003) that the S631A mutant did not alter the hERG VSD mode shift as measured using gating currents. It does not, however, completely rule out the link between entry into the C-type inactivated state and the mode shift. We have previously shown, using a thermodynamic analysis, that the region of the hERG protein where the S631 residue is located is involved very late in the inactivation process (Wang et al., 2011). It is possible therefore that in a multistep inactivation process, the S631A mutation affects a step after that which is a prerequisite for the mode shift.

A second hypothesis in regard to the mode shift in voltage-gated channels is that it occurs as a result of the mechanical load placed on the VSDs by the pore (Haddad and Blunck, 2011). Although our data do not provide any direct evidence for this, they do not exclude the possibility. Our results indicate that even in the background of N-terminal modification, there is tight coupling of the VSD and gate during activation. During deactivation, modification or deletion of the N terminus uncouples the gate from VSD motion. This could imply that there is a different load on the VSD from the gate, but there could be interactions between the VSD and other parts of the pore that remain in tact. Furthermore, in the presence of N-terminal truncation, we do see slightly faster VSD return (albeit much slower than ionic current deactivation). This altered rate of return could also occur as a result of a change in load on the VSD when it is uncoupled. Therefore, although our data give some clues to the mechanism of the VSD mode shift, it is clear that further studies of the molecular players within the VSD and pore domain will be necessary to fully develop our understanding of the intricacies of how VSD mode shifting occurs.

Coupling of the VSD to the cytoplasmic gate

It is widely accepted that during activation of voltagegated channels, upward movement of the VSD in response to depolarization of the transmembrane voltage is coupled to opening of the cytoplasmic activation gate via the S4-S5 linker (Tristani-Firouzi et al., 2002; Long et al., 2005). This short protein domain, the covalent link between the charge carrying S4 and the outermost of the pore domain helices, the S5, makes specific interactions with the distal end of the S6 transmembrane helix to regulate opening of the gate. In several channel types, including hERG, disruption of the specific interactions between the S6 gate and the S4-S5 linker has been shown to uncouple VSD movement from channel opening to some degree. For example, in Shaker, mutations in the S4-S5 (I384N) and S6 (F484G) cause complete separation of the charge-voltage and current-voltage relationships during activation (Haddad and Blunck, 2011), whereas in hERG, the D540K mutant in the S4-S5 linker results in a U-shaped voltage dependence of opening of

the activation gate (Sanguinetti and Xu, 1999; Tristani-Firouzi et al., 2002). However, there is much less understanding about how VSD return is coupled to closing of the activation gate. Certainly to some extent the same domain complexes seem to be involved. The S4-S5 has been implicated in numerous studies, and furthermore, it has been suggested that interactions between the S4-S5 and the N terminus likely contribute to slow deactivation in hERG (Li et al., 2010). Contrary to this however, Van Slyke et al. (2010) showed, using voltage-clamp fluorometry, that mutations in the S4–S5 linker accelerated the rate of voltage sensor return, but this effect was not dependent on the presence of the N terminus. Our data show that modification of the hERG N-terminal tail, either through truncation ($\Delta 2$ –25) or point mutation, uncoupled VSD return from channel deactivation. Although in E518C hERG (a surrogate for wild type) VSD return and current deactivation were coincident, occurring at overlapping voltages, in $\Delta 2$ –25 channels the midpoint for current deactivation was ~40 mV in the depolarized direction compared with the midpoint of VSD return. The kinetics of the deactivation process also supported this uncoupling effect. In E518C channels, the fast component of the rate of ionic current deactivation/gate closing occurred on an identical time scale to VSD return, consistent with this being the rate-limiting factor in gate closing at negative voltages where the fast component is dominant. In contrast, gate closing occurs approximately six times faster than VSD return at all voltages in $\Delta 2$ –25 channels. As well as further demonstrating uncoupling of gate closure and VSD return, this relationship suggests a possible molecular basis for the biphasic time course of hERG deactivation. The first, fast component appears to be related to return of the VSD and is dominant at more negative potentials, whereas a second component, slower in the wild-type channel, may relate to an endogenous voltage-sensitive rearrangement of the cytoplasmic gate.

As an important aside, this disconnect of the effects of N-terminal modification (whether truncation or point mutation) on ionic currents and the fluorescent signal goes some way to answering a question posed by Smith and Yellen (2002) in regard to whether the signal from fluorescent probes bound to this region reflects movement of the VSD or opening of the gate. The fact that modifications of the N terminus of the hERG channel significantly shift the voltage dependence of deactivation of ionic current, representing closing of the gate, while leaving the voltage dependence of the fluorescent signal unaltered indicates that the fluorescent signals do not report opening/closing of the gate, but rather movement of the VSD.

What is the nature of coupling of the VSD to gate?

Our kinetic and equilibrium data support the idea that the N-terminal truncation has uncoupled VSD mode shifting from the cytoplasmic gate. In $\Delta 2$ –25, VSD mode shifting still occurs, but the gate closes faster than the VSD returns and over a different range of holding potentials. This is the first time that uncoupling of this nature has been reported. A previous study in Shaker has showed that mutation in the S4-S5/S6 regions uncouples the VSD from the gate, but in this case the mode shift of the VSD was abolished (Haddad and Blunck, 2011). The authors explain this in terms of the reduction in load on the VSD (as a result of uncoupling from the activation gate) reducing the propensity of the VSD to mode shift. So what distinguishes these two types of uncoupling that result in very different outcomes? Our data show that N-terminal truncation does not affect the activation process, suggesting two separate pathways with separate sets of interactions for activation and deactivation: First, the previously reported S4-S5 interactions with the gate couple VSD upward movement to gate opening, and second, a set of interactions facilitated by the N-terminal tail couple return of the modeshifted VSD to closing of the gate.

With this in mind, what is the nature of the coupling between the VSD and gate during deactivation? It is clear from the literature that during activation the VSD is coupled to the gate via the S4-S5 linker (Sanguinetti and Xu, 1999; Tristani-Firouzi et al., 2002; Long et al., 2005), so it is tempting to speculate that during deactivation, the same complex stays intact. However, as discussed above (Figs. 2, 4, and 6), deletion or point mutation of the N-terminal tail uncouples the VSD from the gate, suggesting the S4-S5, in the absence of the tail, dissociates from its site of interaction on the S6 gate. Perhaps the simplest interpretation then would be that after activation, as the VSD mode shifts, the S4-S5 changes conformation such that specific interactions with the gate are disrupted. The N terminus then binds to this relaxed conformation to couple it to the gate and regulate deactivation.

Regulation of slow deactivation in hERG channels by the N-terminal tail

Our data support the well-reported phenomenon that the N-terminal tail of hERG channels plays a role in regulation of gating. In particular, deletion of the N terminus ($\Delta 2$ –373 and $\Delta 2$ –354), the EAG domain ($\Delta 1$ –135) alone, or short sections of the N-terminal tail before the PAS domain ($\Delta 2$ –9, $\Delta 2$ –16, and $\Delta 2$ –25) accelerates the rates of deactivation (Schönherr and Heinemann, 1996; Spector et al., 1996; Morais Cabral et al., 1998; Wang et al., 1998; Ng et al., 2011). However, none of these studies has examined the effect of these deletions on the voltage-dependent equilibrium of deactivation. We have demonstrated for the first time that in addition to accelerating the rate of channel closure, deletion of the N-terminal 25 aa effectively shifts the voltage-dependent equilibrium of the process in the depolarized direction

relative to wild-type by eliminating the transfer of VSD mode shift to the gate.

So how does the N terminus of hERG act to regulate deactivation gating? The exact binding partner of the N-terminal tail within the relaxed conformation is something we did not seek to identify in this study, though our characterization of the specific residues within the tail which contribute to coupling gives us some clues. The triplet of amino acids with the most significant contribution to coupling are R4-R5-G6, the same basic region identified by Muskett et al. (2011) as contributing to regulating rates of deactivation in hERG. The clustering of positive charge in this region suggests it might interact with either an acidic residue/ patch via charge-charge interaction or alternatively via π -cation interaction with an aromatic residue. In this regard, Muskett et al. (2011) identified an acidic patch on the cyclic nucleotide-binding domain (residues 843, 847, 850, 857, and 864) as a potential site for interaction. Alternatively, the S4-S5 linker contains both acidic (D540 and E544) and aromatic (Y542 and Y545) residues, and this region has been proposed to be the site of interaction for the N-terminal tail in previous studies (Li et al., 2010; De la Peña et al., 2011). Furthermore, our own data has previously identified the S4-S5 linker as a signal integrator with a dual role in activation and deactivation, i.e., the S4-S5 makes separate sets of interactions in the open and closed states, and that Y545 in particular perturbed rates of deactivation. Either of these regions therefore has potential to be the site of interaction for the N-terminal tail that governs coupling during deactivation.

Although our analysis cannot answer the question of molecular interactions directly, it does give some insight into which states of the channel complex the N-terminal tail interacts with. Two pieces of evidence from our data point toward the N terminus interacting with an open channel state, stabilizing an interaction between the VSD and open gate. First, truncation of the tail does not affect activation (i.e., does nothing to the forward reaction). Second, truncation reduces the energy requirement of the open to closed transition (less change in transmembrane potential is required to return the VSD to the down conformation in $\Delta 2-25$ compared with E518C), suggesting the presence of the tail stabilizes the open state. This fits with the observation by Wang et al. (1998) that exogenous application of a peptide corresponding to the first 16 aa stabilized an open state of the channel in single channel experiments. Further to this, a recent study in Ci-VSP has suggested three conformations for VSDs (Villalba-Galea et al., 2008): resting, active, and relaxed, where the transition from active to relaxed as the VSD forms additional interactions to stabilize the up conformation is thought to be responsible for the mode shift observed after sustained depolarization. The authors suggest that as the most stable up state, the relaxed conformation is the one that has been observed in crystal structures of voltage-gated ion channels. Our data are consistent with the likelihood that of the two up states of the VSD, the N-terminal tail of hERG interacts with the relaxed state to regulate slow deactivation. Two potential arguments point toward this conclusion, the first of them is a question of probability. If VSD relaxing/mode shifting does correlate with entry to the C-type inactive state, then based on the kinetics of hERG channels, this would imply that the VSD activated conformation, although most likely the dominant functional conformation in slower inactivating channels, is extremely transient in hERG. For example at 40 mV, the rate of VSD upward movement occurs with a time constant of \sim 200 ms (Fig. 3), whereas inactivation in hERG occurs \sim 100-fold faster at this potential (Wang et al., 1997). As a result, the equilibrium occupation of activated versus relaxed VSD conformations at depolarized potentials is heavily weighted toward relaxed, suggesting this as the most likely of the up conformations of the VSD to interact with the N-terminal tail. The second argument for the N-terminal tail interacting with the relaxed VSD is that the kinetics and voltage sensitivity of gate closing in the presence of the N-terminal tail clearly mirror those of the relaxed VSD, suggesting the complex in which the N-terminal tail is involved includes the relaxed conformation.

A final clue into how the N terminus may regulate deactivation can be drawn from another important observation from the literature. Wang et al. (2000) reported that injection of a peptide corresponding to the first 16 aa was capable of reestablishing slow deactivation in N-terminal truncated core hERG mutants expressed in oocytes. Although the authors do not report any effects on the mode shift, they suggest the N-terminal is involved in stabilization of a complex of interacting domains rather than exerting a mechanical regulatory effect on the open channel complex. That is, because

the exogenous peptide is not connected to any other channel domains, it cannot exert any force on the VSD/gate/X domain complex itself, but rather provides an interaction point or glue to stabilize the activated complex. For example, in this case the VSD might interact with one part of the peptide and the gate with another.

Based on these observations, Fig. 8 presents a possible domain level view of the complexes formed between the N-terminal tail, the VSD, the S4-S5, and the gate that are involved in regulating hERG gating. Although we cannot presume this to be the exact nature of the interactions, it represents perhaps the simplest interpretation of the data and provides a framework for consideration of the differential coupling of VSD motion to the gate in hERG activation/deactivation. In this scenario, the S4-S5 has two conformations, associated with the up and down states of the VSD. In the down state, the S4-S5 directly binds the S6 gate to couple VSD upward motion to opening of the gate. In the up (relaxed) VSD conformation, the S4-S5 orientation has altered such that it is no longer positioned to make direct contact with the gate but requires the presence of the N-terminal tail as an adaptor to couple VSD return to gate closure.

Summary

The data we have presented here describe several novel features of hERG gating. We have demonstrated that mode shifting of the hERG VSD results in a corresponding shift in the voltage-dependent equilibrium of channel opening/closing and that at negative potentials, coupling of the mode-shifted VSD to the gate defines the rate of channel closure. We have shown that deletion of the first 25 aa from the N terminus of hERG uncouples the gate from the VSD during deactivation but not activation and proposed a dual mechanism of coupling of the VSD to the gate in hERG channels. Furthermore, we have demonstrated that a

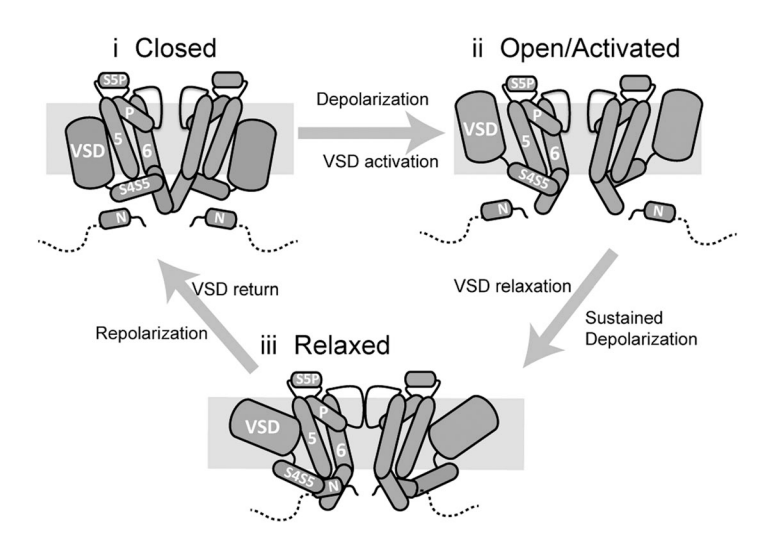


Figure 8. A simple domain level model of coupling of VSD mode shifting to the gate during hERG activation/deactivation. (i) In the closed state, the N-terminal tail does not directly interact with the gate. (ii) Upon depolarization, the VSD moves in the membrane into the activated state. This upward motion is coupled to opening of the gate via direct interactions of the S4–S5 and the S6 helix. (iii) With sustained depolarization, the VSD relaxes. Relaxation of the VSD is accompanied by a conformational change of the S4–S5 linker that causes it to dissociate from its binding site on the S6. The N-terminal tail then acts as an adaptor between the S4–S5 and S6 to couple VSD return during repolarization to closing of the gate.

triplet of residues in the unstructured region of the N-terminal tail, R4, R5, and G6, are the primary contributors to coupling of VSD return to closing of the gate. Physiologically, the mode shifting reported here is significant in terms of the contribution of hERG channels to repolarization of the cardiac action potential. For each heart beat, the action potential typically has a duration of 200-300 ms (Nerbonne and Kass, 2005). Mode shifting in hERG occurs over a similar time scale, meaning the membrane potential dwells at depolarized potentials long enough for the process to occur. As a result, during repolarization, hERG channels deactivate over a more hyperpolarized voltage range to which they activate during depolarization. This shift would maximize the contribution of hERG channels to repolarization (because channels would close at more negative potentials later in the action potential), as well as maintaining channel availability over a longer period for suppression of premature beats (Lu et al., 2001).

We thank Tadeusz Marciniec for technical assistance.

This work was funded by grants from the Australian Research Council (DP0986316), the National Health and Medical Research Council (459401 and 1010029), and the National Heart Foundation of Australia (G09S-450). A.P. Hill is an Australian Research Council Future Fellow and J.I. Vandenberg is a National Health and Medical Research Council Senior Research Fellow.

Kenton J. Swartz served as editor.

Submitted: 19 December 2011 Accepted: 23 July 2012

REFERENCES

- Barros, F., D. del Camino, L.A. Pardo, T. Palomero, T. Giráldez, and P. de la Peña. 1997. Demonstration of an inwardly rectifying K+ current component modulated by thyrotropin-releasing hormone and caffeine in GH3 rat anterior pituitary cells. *Pflugers Arch.* 435:119–129. http://dx.doi.org/10.1007/s004240050491
- Bezanilla, F., R.E. Taylor, and J.M. Fernández. 1982. Distribution and kinetics of membrane dielectric polarization. 1. Long-term inactivation of gating currents. *J. Gen. Physiol.* 79:21–40. http://dx.doi.org/10.1085/jgp.79.1.21
- Bruening-Wright, A., and H.P. Larsson. 2007. Slow conformational changes of the voltage sensor during the mode shift in hyperpolarization-activated cyclic-nucleotide-gated channels. *J. Neurosci.* 27:270–278. http://dx.doi.org/10.1523/JNEUROSCI.3801-06.2007
- Clarke, C.E., A.P. Hill, J. Zhao, M. Kondo, R.N. Subbiah, T.J. Campbell, and J.I. Vandenberg. 2006. Effect of S5P alpha-helix charge mutants on inactivation of hERG K+ channels. *J. Physiol.* 573:291–304. http://dx.doi.org/10.1113/jphysiol.2006.108332
- de la Peña, P., C. Alonso-Ron, A. Machín, J. Fernández-Trillo, L. Carretero, P. Domínguez, and F. Barros. 2011. Demonstration of physical proximity between the N terminus and the S4-S5 linker of the human ether-a-go-go-related gene (hERG) potassium channel. *J. Biol. Chem.* 286:19065–19075. http://dx.doi.org/10.1074/jbc.M111.238899
- Haddad, G.A., and R. Blunck. 2011. Mode shift of the voltage sensors in Shaker K⁺ channels is caused by energetic coupling to the pore domain. *J. Gen. Physiol.* 137:455–472. http://dx.doi.org/10.1085/jgp.201010573

- Li, Q., S. Gayen, A.S. Chen, Q. Huang, M. Raida, and C. Kang. 2010. NMR solution structure of the N-terminal domain of hERG and its interaction with the S4-S5 linker. *Biochem. Biophys. Res. Commun.* 403:126–132. http://dx.doi.org/10.1016/j.bbrc.2010.10.132
- Long, S.B., E.B. Campbell, and R. Mackinnon. 2005. Voltage sensor of Kv1.2: structural basis of electromechanical coupling. *Science*. 309:903–908. http://dx.doi.org/10.1126/science.1116270
- Lu, Y., M.P. Mahaut-Smith, A. Varghese, C.L. Huang, P.R. Kemp, and J.I. Vandenberg. 2001. Effects of premature stimulation on HERG K(+) channels. *J. Physiol.* 537:843–851. http://dx.doi.org/10.1113/jphysiol.2001.012690
- Morais Cabral, J.H., A. Lee, S.L. Cohen, B.T. Chait, M. Li, and R. Mackinnon. 1998. Crystal structure and functional analysis of the HERG potassium channel N terminus: a eukaryotic PAS domain. *Cell*. 95:649–655. http://dx.doi.org/10.1016/S0092-8674(00)81635-9
- Muskett, F.W., S. Thouta, S.J. Thomson, A. Bowen, P.J. Stansfeld, and J.S. Mitcheson. 2011. Mechanistic insight into human ether-à-go-go-related gene (hERG) K+ channel deactivation gating from the solution structure of the EAG domain. J. Biol. Chem. 286:6184–6191. http://dx.doi.org/10.1074/jbc.M110.199364
- Nerbonne, J.M., and R.S. Kass. 2005. Molecular physiology of cardiac repolarization. *Physiol. Rev.* 85:1205–1253. http://dx.doi.org/10.1152/physrev.00002.2005
- Ng, C.A., M.J. Hunter, M.D. Perry, M. Mobli, Y. Ke, P.W. Kuchel, G.F. King, D. Stock, and J.I. Vandenberg. 2011. The N-terminal tail of hERG contains an amphipathic α-helix that regulates channel deactivation. *PLoS ONE*. 6:e16191. http://dx.doi.org/10.1371/journal.pone.0016191
- Olcese, R., R. Latorre, L. Toro, F. Bezanilla, and E. Stefani. 1997. Correlation between charge movement and ionic current during slow inactivation in *Shaker* K⁺ channels. *J. Gen. Physiol.* 110:579–589. http://dx.doi.org/10.1085/jgp.110.5.579
- Pathak, M.M., V. Yarov-Yarovoy, G. Agarwal, B. Roux, P. Barth, S. Kohout, F. Tombola, and E.Y. Isacoff. 2007. Closing in on the resting state of the Shaker K(+) channel. *Neuron*. 56:124–140. http://dx.doi.org/10.1016/j.neuron.2007.09.023
- Perrin, M.J., R.N. Subbiah, J.I. Vandenberg, and A.P. Hill. 2008. Human ether-a-go-go related gene (hERG) K+ channels: function and dysfunction. *Prog. Biophys. Mol. Biol.* 98:137–148. http://dx.doi.org/10.1016/j.pbiomolbio.2008.10.006
- Piper, D.R., A. Varghese, M.C. Sanguinetti, and M. Tristani-Firouzi. 2003. Gating currents associated with intramembrane charge displacement in HERG potassium channels. *Proc. Natl. Acad. Sci. USA*. 100:10534–10539. http://dx.doi.org/10.1073/pnas.1832721100
- Sanguinetti, M.C., and Q.P. Xu. 1999. Mutations of the S4-S5 linker alter activation properties of HERG potassium channels expressed in Xenopus oocytes. *J. Physiol.* 514:667–675. http://dx.doi.org/ 10.1111/j.1469-7793.1999.667ad.x
- Sanguinetti, M.C., C. Jiang, M.E. Curran, and M.T. Keating. 1995.
 A mechanistic link between an inherited and an acquired cardiac arrhythmia: HERG encodes the IKr potassium channel. *Cell*. 81:299–307. http://dx.doi.org/10.1016/0092-8674(95)90340-2
- Schönherr, R., and S.H. Heinemann. 1996. Molecular determinants for activation and inactivation of HERG, a human inward rectifier potassium channel. *J. Physiol.* 493:635–642.
- Smith, P.L., and G. Yellen. 2002. Fast and slow voltage sensor movements in HERG potassium channels. *J. Gen. Physiol.* 119:275–293. http://jgp.rupress.org/content/119/3/275
- Smith, P.L., T. Baukrowitz, and G. Yellen. 1996. The inward rectification mechanism of the HERG cardiac potassium channel. *Nature*. 379:833–836. http://dx.doi.org/10.1038/379833a0
- Spector, P.S., M.E. Curran, A. Zou, M.T. Keating, and M.C. Sanguinetti. 1996. Fast inactivation causes rectification of the IKr channel. J. Gen. Physiol. 107:611–619. http://dx.doi.org/10.1085/jgp.107.5.611

- Tristani-Firouzi, M., J. Chen, and M.C. Sanguinetti. 2002. Interactions between S4-S5 linker and S6 transmembrane domain modulate gating of HERG K+ channels. *J. Biol. Chem.* 277:18994–19000. http://dx.doi.org/10.1074/jbc.M200410200
- Trudeau, M.C., J.W. Warmke, B. Ganetzky, and G.A. Robertson. 1995. HERG, a human inward rectifier in the voltage-gated potassium channel family. *Science*. 269:92–95. http://dx.doi.org/10.1126/science.7604285
- Van Slyke, A.C., S. Rezazadeh, M. Snopkowski, P. Shi, C.R. Allard, and T.W. Claydon. 2010. Mutations within the S4-S5 linker alter voltage sensor constraints in hERG K+ channels. *Biophys. J.* 99:2841–2852. http://dx.doi.org/10.1016/j.bpj.2010.08.030
- Villalba-Galea, C.A., W. Sandtner, D.M. Starace, and F. Bezanilla. 2008. S4-based voltage sensors have three major conformations. *Proc. Natl. Acad. Sci. USA*. 105:17600–17607. http://dx.doi.org/10.1073/pnas.0807387105
- Wang, D.T., A.P. Hill, S.A. Mann, P.S. Tan, and J.I. Vandenberg. 2011. Mapping the sequence of conformational changes under-

- lying selectivity filter gating in the K(v)11.1 potassium channel. *Nat. Struct. Mol. Biol.* 18:35–41. http://dx.doi.org/10.1038/nsmb.1966
- Wang, J., M.C. Trudeau, A.M. Zappia, and G.A. Robertson. 1998. Regulation of deactivation by an amino terminal domain in human ether-à-go-go-related gene potassium channels. J. Gen. Physiol. 112:637–647. http://dx.doi.org/10.1085/jgp.112.5.637
- Wang, J., C.D. Myers, and G.A. Robertson. 2000. Dynamic control of deactivation gating by a soluble amino-terminal domain in *HERG* K(⁺) channels. *J. Gen. Physiol.* 115:749–758. http://dx.doi.org/10.1085/jgp.115.6.749
- Wang, S., S. Liu, M.J. Morales, H.C. Strauss, and R.L. Rasmusson. 1997. A quantitative analysis of the activation and inactivation kinetics of HERG expressed in *Xenopus* oocytes. *J. Physiol.* 502: 45–60. http://dx.doi.org/10.1111/j.1469-7793.1997.045bl.x
- Wonderlin, W.F., and J.S. Strobl. 1996. Potassium channels, proliferation and G1 progression. *J. Membr. Biol.* 154:91–107. http://dx.doi.org/10.1007/s002329900135REFERENCE